

A continuous hemodynamic parameters algorithm based on the wearable tonometric device

Jiayuan Fang^{1,2}, Siyuan Zhou^{1,2}, Ye Miao³, Chentao Du^{1,2,4,5}, Binyang Ding^{1,2}, Mengkang Deng^{1,2}, Tingrui Pan^{1,2,*}

Abstract— This study introduces a pioneering approach to managing hypertension and preventing catastrophic cardiovascular events through a novel continuous hemodynamics algorithm, integrated within a wearable tonometric device (WTD). This advanced algorithm leverages mathematical analysis of arterial pressure (AP) waveforms, accurately calculating key hemodynamic parameters such as systolic blood pressure (SBP), diastolic blood pressure (DBP), mean blood pressure (MBP), and heart rate (HR). These calculations are performed in real time by identifying feature points in AP waveforms and extracting vital parameters through pulse wave analysis (PWA). The algorithm incorporates pre-input biometric data to create a data vector, which is then processed using a multiple non-linear regression model to compute beat-to-beat Cardiac output (CO). Additional hemodynamic parameters are derived by analyzing pulse waveforms in conjunction with CO values, ensuring a comprehensive hemodynamic profile. The efficacy and precision of this algorithm are validated against commercial medical-grade devices and the WTD system through human trials, demonstrating medical-grade accuracy. The results affirm the stability, reliability, and accuracy of the hemodynamic parameters algorithm, highlighting the WTD's potential as a transformative solution in wearable health technology. By providing real-time, medical-grade monitoring in a wearable format, the WTD device is set to revolutionize remote patient-centered healthcare, offering a proactive approach to monitoring and managing cardiovascular health.

I. INTRODUCTION

Cardiovascular diseases, notably hypertension, are the primary global cause of mortality[1]. The surveillance of hypertension is increasingly vital in preventing, treating, and managing postoperative cardiovascular diseases[2]. Consequently, the precise measurement of blood pressure (BP) and other essential hemodynamic parameters is crucial for clinical diagnosis, treatment evaluation, prevention of complications, and reducing the risk of cardiovascular diseases[3]. Invasive arterial catheterization is widely regarded as the gold standard for hemodynamic assessment due to its high level of accuracy[4]. However, it also carries the risk of infection and injury. Non-invasive methods, such as auscultation and oscillometry, are safer and widely used but offer only intermittent measurements[5]. Techniques like echocardiography provide continuous monitoring but are

unsuitable for long-term or self-monitoring. Volume clamp and applanation tonometry present continuous alternatives but face challenges in practical application for outpatient settings due to discomfort and complexity[6]. Accurate monitoring is critical to management, but existing invasive measurements and non-invasive techniques both have limitations, necessitating the need for better continuous monitoring solutions.

Advancements in flexible electronics have paved the way for wearable devices to transform hemodynamic monitoring[7]. This study introduces the WTD system, a novel, fully wearable hemodynamic monitoring device equipped with an adaptive, highly sensitive, and flexible iontronic sensing (FITS) array for continuous, dynamic hemodynamic parameters assessment. The WTD system, leveraging a highly sensitive and spatially precise FITS, automates vessel localization and applanation, enhancing arterial pressure waveform accuracy. This device enables the capture of high-precision pulse waveforms, leading to the development of an algorithm designed for continuous blood pressure and multi-parametric monitoring (HR, CO, etc.), ensuring medical-grade precision in a wearable format. The WTD is expected to transform clinical monitoring, shifting the focus from hospital settings to home-care environments, and marks a significant advancement in patient-centered hemodynamic monitoring.

II. METHODS

Invented in the 1950s, the applanation tonometry was later adopted to measure dynamic arterial blood pressure similarly to assessing intraocular pressure[8]. Specifically, the device needs to be placed over a superficial artery that is supported by a physiologically stiff structure beneath, e.g., a bone. Therefore, the radial artery at the wrist has been determined as a desired matching site. We have developed a wrist wearable tonometric device, the optical image of which is shown in Fig. 1A. The WTD leverages a FITS technology-based tactile sensor (Fig. 1B) and streamlines the traditional biaxial search for pulse waveforms, enhancing intra-arterial pressure determination. As shown in Fig. 1C, the WTD can be conformably attached to human skin and fit to the curvature of the wrist. The lateral dimension of each element in the WTD is designed to be 1mm, less than half the arterial diameter.

¹ School of Biomedical Engineering, Division of Life Sciences and Medicine, University of Science and Technology of China, Hefei, Anhui, 230026, P.R China {tingrui@ustc.edu.cn}

² Suzhou Institute for Advanced Research, University of Science and Technology of China, Suzhou, Jiangsu, 215123, P.R China

³ School of Mechanical and Electrical Engineering, Soochow University, Suzhou 215000, China

⁴ Department of Biomedical Engineering, City University of Hong Kong, Hong Kong, 999077, China

⁵ Hong Kong Centre for Cerebro-Cardiovascular Health Engineering, Hong Kong, 999077, China

(approximately 2-3 mm in diameter[9]), ensuring that there is always at least one measuring unit positioned right above the flattened radial artery, leading to accurate detection of AP waveforms. The WTD uses signal analysis and a high-precision step-motor for targeted applanation, enabling continuous blood pressure monitoring through efficient one-dimensional scanning.

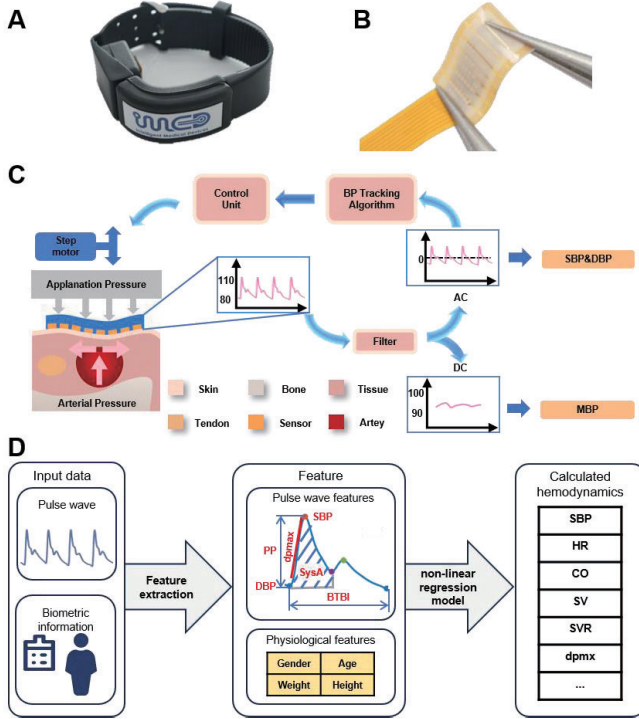


Figure 1. (A) Optical images of the WTD. (B) Optical images of the FITS array. (C) Diagram of the operating principle of the WTD. (D) Block diagram of the flow of multiple nonlinear regression modeling to compute CO.

Importantly, for non-invasive continuous blood pressure monitoring, the pulse waveform signals sensed by the skin surface sensors are not equal to the blood pressure values inside the blood vessels[10]. As a result, calibration becomes an essential procedure. Similar to the oscillometric method which is used as a standard calibration technique for continuous hemodynamic monitoring, the WTD extracts the oscillometric envelope and the information of the pressure with the increasing pressure level, from which MBP, SBP and DBP can be directly determined[11]. With the motorized mechanical unit to load on the vascular structure, the WTD includes the capacity to calibrate itself to the intra-arterial blood pressure without any external apparatus. Utilizing the initial blood pressure values acquired during the calibration procedure, the continuous blood pressure can be calculated based on the AP waveforms at the targeted applanation level, as follows:

$$P_{BP} = P_{DC} + P_{AC} \cdot \frac{SBP_{init} - DBP_{init}}{P_{ACmax} - P_{ACmin}} \quad (1)$$

Where P_{BP} is the continuous blood pressure; P_{DC} and P_{AC} stand for the static and pulsed components of P_{BP} , respectively; SBP_{init} and DBP_{init} represent the initial systolic and diastolic blood pressure values obtained from the calibration process, and P_{ACmax} and P_{ACmin} indicate the peak and trough of P_{AC} , respectively.

After the AP waveforms are calibrated, the corresponding blood pressure and other important hemodynamic parameters variations can be analyzed by using calibrated AP waveforms. Specifically, pulse wave analysis (PWA) is used in the WTD system to continuously estimate a series of hemodynamic parameters by mathematically analyzing the AP waveforms[12]. After passing through an analog filter, the calibrated pulse waveforms can be extracted into both static and pulsed components. In our study, the cutoff frequency used for separating dynamic and static pressure is 0.5 Hz.

As depicted in Fig. 1D, five feature points in the beat-to-beat pulse waveform can be continuously detected in real-time by the algorithm, identified as the pulse wave begin, the pulse wave end, the systolic peak, the diastolic notch, and the diastolic peak. After that, the SBP, DBP, MBP, pulse pressure (PP), beat-to-beat interval (BTBI), SysA and maximum slope of the arterial pulse curve within the systole (dPmax) are extracted based on the above feature parameters. SysA is the area under the arterial waveform curve within systole; SV is proportional to the area under the systolic portion of the arterial AP waveform[13]; and dPmax represents the maximum slope of the arterial pulse curve during systole, which closely approximates the contractility of the left ventricle. Together with the pre-input biometric information (gender, age, height, weight), the input source data vector was formed, and the beat-to-beat CO can be calculated by a mathematical model of multiple non-linear regression[14]. Then, other hemodynamic parameters can be calculated from the pulse waveforms and CO values. The statistical formulas mentioned can be seen in Table 1.

Table 1. Calculation of other essential hemodynamic parameters

Abbreviation	Complete name	Calculation Formula
SV (mL/beat)	stroke volume	$SV = CO / (HR \times 1000)$
SVR (mL/baet)	systemic vascular resistance	$SVR = 80 \times (MAP - RAP) / CO$
CI (L/(min·m ²))	Cardiac index	$CI = CO / BSA$
SI (mL/(beat·m ²))	stroke volume index	$SVI = SV / BSA$
CPO (W)	Cardiac power output	$CPO = MAP \times CO$
SVV (%)	stroke volume variation	$SVV(\%) = 100 \times [(SV_{max} - SV_{min}) / SV_{mean}]$
PPV (%)	pulse pressure variation	$PPV(\%) = 100 \times [(PP_{max} - PP_{min}) / PP_{mean}]$

$$*BSA (m^2) = 0.0061 \times \text{height(cm)} + 0.0128 \times \text{weight(kg)} - 0.1529$$

III. RESULT

To verify the accuracy of the hemodynamic algorithm, we conducted tests on 10 subjects with the commercial medical-grade device (TL-400, Tensys Medical). Specifically, AP

waveforms and CO values were collected with the TL-400, and our algorithm was applied to these waveforms to calculate CO values, which were then validated against the TL-400's medical-grade readings. Fig. 2A illustrates the efficacy of the algorithm in recognizing feature points of the pulse wave and accurately locating each characteristic. As shown in Fig. 2B, the CO data ranged from 1.5 to 12 L/min, covering the majority of the CO range. Moreover, color coding is employed to represent measurements from the same subject, showing a mean difference of -0.04 ± 0.51 L/min between TL-400 and calculated CO values. Additionally, the CO calculation's percentage error (PE) is 11.23%, well within the 30% clinical acceptability [15]. Furthermore, a high consistency between TL-400 and calculated CO is observed in Fig. 2C.

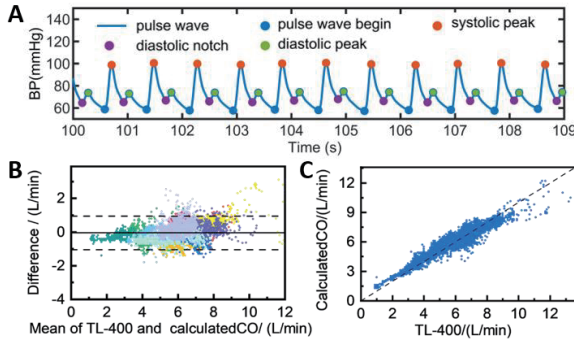


Figure 2. (A) Identification of pulse wave characteristic points; (B) Bland-Altman plot for CO with points color-coded by subjects; (C) Correlation of CO measurements between TL-400 and calculated CO.

Additionally, to evaluate the quality of the AP waveforms at the desired appplanation level, we employed both the WTD and the TL-400 devices to acquire and compare the AP waveforms from one subject. Fig. 3A demonstrates that AP waveforms collected simultaneously by the WTD and the TL-400 exhibit no significant differences in the time domain. Fig. 3B shows the normalized pulse waveforms, with the light and black lines representing the superimposed waveforms and their average, respectively. Relative errors ranging from 0.021 to 0.052 illustrate the beat-to-beat precision of WTD measurements qualitatively.

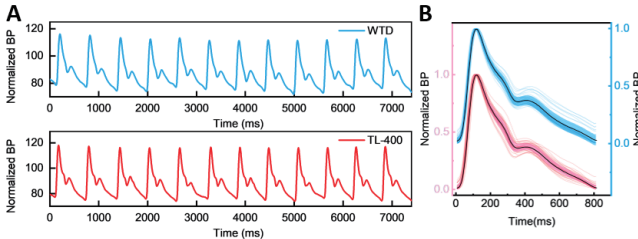


Figure 3. (A) Example of AP waveforms measured by the WTD and the TL-400. (B) Superimposed normalized beat-to-beat AP waveforms from the WTD (blue line) and the TL-400 (red line) from the same subject.

After initial verification of the accuracy and effectiveness of the hemodynamic calculation algorithm, it was deployed on the WTD for continuous hemodynamic monitoring. The high-precision AP waveforms detected by the WTD can

subsequently be utilized through this algorithm to continuously compute key hemodynamic parameters, including BP, HR, and CO, as described in the Methods section. To validate the accuracy of continuous hemodynamic parameters monitoring with the WTD, we applied the TL-400 and the WTD devices to a healthy subject and performed heart rate validation with standard 3-lead ECG electrodes.

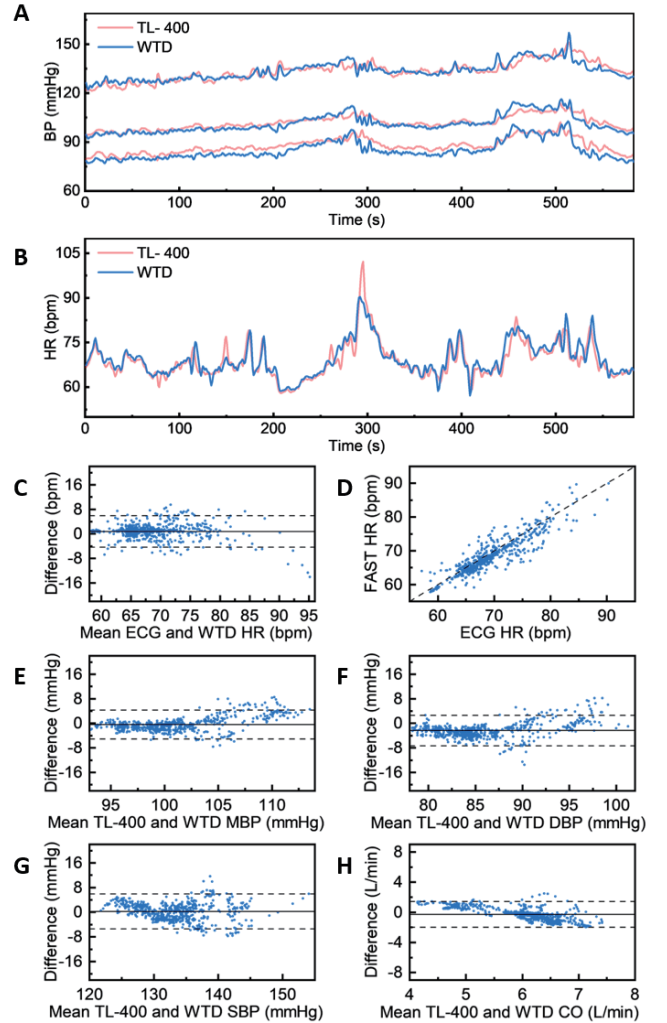


Figure 4. (A) SBP, MBP and DBP data derived by the WTD and the TL-400. (B) HR data derived by the WTD and the TL-400. (C) Bland-Altman plot of HR comparison between the WTD and the ECG devices. (D) Linear correlation diagram of HR comparison between the WTD and the ECG devices. (E) Bland-Altman plot of MBP comparison between the WTD and the TL-400. (F) Bland-Altman plot of DBP comparison between the WTD and the TL-400. (G) Bland-Altman plot of SBP comparison between the WTD and the TL-400. (H) Bland-Altman plot of CO comparison between the WTD and the TL-400.

The evaluation of blood pressure measurements is conducted first. Fig. 4A shows the MBP, DBP and SBP data continuously measured by the WTD and the TL-400 from the subject. To further evaluate the accuracy and precision of the beat-to-beat blood pressure measurement, Bland-Altman

analysis is performed to assess the measurement differences between the WTD and the TL-400. Figs. 4E-G illustrate the derived mean biases in the comparative analysis of MBP, DBP, and SBP between the WTD and the TL-400, where the dashed lines demarcate the 95% confidence interval for the limits of agreement. In particular, the mean differences and the standard deviations of MBP, DBP and SBP are -0.33 ± 2.40 mmHg, -2.35 ± 2.56 mmHg and 0.26 ± 2.90 mmHg, respectively. These values are well within the limits of 5 ± 8 mmHg set by the AAMI[16]. Therefore, the comparison results suggest that the WTD is capable of measuring blood pressure within the medical-grade precision.

The beat-to-beat heart rate monitoring capability of the WTD is evaluated in the subsequent data analysis by comparing its measurements with simultaneous ECG recordings. Fig. 4B shows the continuous HR measurements taken from the same individual using both the WTD and ECG devices over 10 minutes. Furthermore, the mean difference and standard deviation between the WTD system and ECG measurements are 0.81 ± 2.60 BPM as shown in Fig. 4C. The data plotted in Fig. 4D exhibits a high correlation, with a correlation coefficient of 0.97. These results indicate that the HR values derived from the WTD have a high statistical precision compared to that of the clinical gold standard and are compliant with the published standard[17], which defines an acceptable accuracy within ± 5 bpm.

Finally, the estimation of the measurement of CO is shown in Fig. 4H, the mean of the differences and the standard deviations between the WTD and the TL-400 are -0.27 ± 0.88 L/min, and the PE of the CO values between the WTD and the TL-400 is 28.6%, which meets the acceptable clinical agreement of the CO measurement devices [15]. In conclusion, the above measurements are all within the required accuracy of the clinical standards. The hemodynamic parameters algorithm has been demonstrated to be deployable on wearable tonometric devices, continuously tracking key hemodynamic parameters including HR, BP, and CO within medical-grade accuracy.

IV. CONCLUSION

In summary, a novel hemodynamics calculation algorithm has been developed for continuous wearable real-time assessments of hemodynamic parameters with medical-grade precision, which has been successfully deployed on a wearable tonometric device. Specifically, the algorithm can separate the pulse waveforms collected by the WTD into static and pulsed pressure components, and continuously extract characteristic points from the pulse wave signals. Subsequently, by integrating biometric information of the subjects, the algorithm employs a multiple non-linear regression model to enable real-time monitoring of BP, CO, and other hemodynamic parameters. In the clinical validation experiments, the algorithm has demonstrated its high accuracy and reliability in measuring key hemodynamic parameters which is of great significance for improving patient prognosis and optimizing cardiovascular intervention.

ACKNOWLEDGMENT

The authors thank Yonghua Li, and Tao Li for their support on the hardware designs of the system.

REFERENCES

- [1] E. G. Nabel, "Cardiovascular Disease," *N Engl J Med*, vol. 349, no. 1, pp. 60–72, Jul. 2003.
- [2] J. B. Kostis, "The Importance of Managing Hypertension and Dyslipidemia to Decrease Cardiovascular Disease," *Cardiovasc Drugs Ther*, vol. 21, no. 4, pp. 297–309, Sep. 2007.
- [3] H. O. Ventura, S. J. Taler, and J. E. Strobeck, "Hypertension as a hemodynamic disease: the role of impedance cardiography in diagnostic, prognostic, and therapeutic decision making," *Am J Hypertens*, vol. 18, no. 2 Pt 2, pp. 26S–43S, Feb. 2005.
- [4] J. Pugsley and A. B. Lerner, "Cardiac Output Monitoring: Is There a Gold Standard and How Do the Newer Technologies Compare?," *Semin Cardiothorac Vasc Anesth*, vol. 14, no. 4, pp. 274–282, Dec. 2010.
- [5] B. S. Alpert, D. Quinn, and D. Gallick, "Oscillometric blood pressure: a review for clinicians," *J. Am. Soc. Hypertens.*, vol. 8, no. 12, pp. 930–938, Dec. 2014.
- [6] H. Tjahjadi and K. Ramli, "Review of photoplethysmography based non-invasive continuous blood pressure methods," in *2017 15th International Conference on Quality in Research: International Symposium on Electrical and Computer Engineering*, Nusa Dua, Bali, Indonesia: IEEE, Jul. 2017, pp. 173–178.
- [7] J. Kim, E. Chou, J. Le, S. Wong, M. Chu, and M. Khine, "Soft Wearable Pressure Sensors for Beat-to-Beat Blood Pressure Monitoring," *Adv Healthcare Materials*, vol. 8, no. 13, p. 1900109, Jul. 2019.
- [8] K. Matthys and P. Verdonck, "Development and modeling of arterial applanation tonometry: A review," *Technology and Health Care*, vol. 10, no. 1, pp. 65–76, Feb. 2002.
- [9] W. Wahood, S. Ghazy, A. Al-Abdulghani, and D. F. Kallmes, "Radial artery diameter: a comprehensive systematic review of anatomy," *J. Neurointerv. Surg.*, vol. 14, no. 12, pp. 1274–1278, Dec. 2022.
- [10] N. P.M., R. K. V., J. Joseph, and M. Sivaprakasam, "Non-Invasive Assessment of Local Pulse Wave Velocity as Function of Arterial Pressure," in *2018 IEEE International Symposium on Medical Measurements and Applications (MeMeA)*, pp. 1–6, Jun. 2018.
- [11] J. Fortin *et al.*, "A novel art of continuous noninvasive blood pressure measurement," *Nat. Commun.*, vol. 12, no. 1, Art. no. 1, Mar. 2021.
- [12] B. Saugel *et al.*, "An autocalibrating algorithm for non-invasive cardiac output determination based on the analysis of an arterial pressure waveform recorded with radial artery applanation tonometry: a proof of concept pilot analysis," *Journal of Clinical Monitoring and Computing*, vol. 28, no. 4, pp. 357–362, Aug. 2014.
- [13] J. X. Sun, A. T. Reisner, M. Saeed, T. Heldt, and R. G. Mark, "The cardiac output from blood pressure algorithms trial," *Critical care medicine*, vol. 37, no. 1, pp. 72–80, Jan. 2009.
- [14] B. Saugel *et al.*, "An autocalibrating algorithm for non-invasive cardiac output determination based on the analysis of an arterial pressure waveform recorded with radial artery applanation tonometry: a proof of concept pilot analysis," *J. Clin. Monit. Comput.*, vol. 28, no. 4, pp. 357–362, Aug. 2014.
- [15] L. A. Critchley and J. A. Critchley, "A meta-analysis of studies using bias and precision statistics to compare cardiac output measurement techniques," *J. Clin. Monit. Comput.*, vol. 15, no. 2, pp. 85–91, Feb. 1999.
- [16] "ANSI/AAMI/ISO 81060-2:2019 - Non-invasive sphygmomanometers - Part 2: Clinical investigation of intermittent automated measurement type," 2019.
- [17] "ANSI/AAMI EC13-2002 - Cardiac Monitors, Heart Rate Meters, and Alarms," 2002.